

Modified Threshold - based Intelligent Enhanced Energy Detector for Cognitive Radio Networks

Narendrakumar Chauhan¹, Sagar Kavaiya², Purvang Dalal³

Submitted: 24/04/2023

Revised: 25/06/2023

Accepted: 04/07/2023

Abstract: This paper introduces an enhanced energy detector (IED) that utilizes the Nakagami-m fading channel with maximal ratio combining (MRC) in multiple-input multiple-output (MIMO) configurations. The main objective of the research is to optimize the performance of a cognitive radio (CR) system consisting of N unlicensed user (SU) and one licensed user (PU). By employing Kummer's solution for CR, the expressions for the likelihood of miss detection are derived for the p-based energy detection (ED) approach. Arithmetic operation on threshold are incorporated in order to improve the efficiency of detection. The effectiveness of the proposed approach is evaluated through error rate analysis, and simulations are conducted to validate the derived expressions. The study also investigates the impact of combined correlated fading and static distance on detection performance in aligned with faulty state information of channel (CSI). Furthermore, the influence of the correlation coefficient is examined through simulations. The results demonstrate that antennas connected in an exponential manner outperform those connected uniformly.

Keywords: Spectrum Sensing, Inter Branch Correlation, Nakagami-m fading channel, Imperfect Channel State Information

1. Introduction

With the growing number of connected users on the road, there is a rising demand for opportunistic allocation of spectrum resources. In dense traffic scenarios, the conventional "Dedicated Short-Range Communication (DSRC)" may prove inadequate in meeting the resource needs due to limitations in data channels. To address this issue, the utilization of (CR) technology becomes necessary in vehicular communication. Spectrum Sensing (SS) is a crucial component of CR, as it involves the identification of vacant primary channels that can be utilized. In this context, the task of spectrum sensing is performed by Secondary Users (SU) [1].

In [2] Author presents the use of ED for SS when dealing with unfamiliar sources. Among various techniques for SS, ED stands out due to its simplicity in implementation, as highlighted in reference [3]. In order to further enhance the detection capabilities of ED, reference [4] proposes a modified version called IED. This modified technique substitutes the squaring operation in ED with a user-defined power value represented as "p." The authors of [4] demonstrate that the utilization of IED yields improved detection performance compared to the original ED method. The author of [4] effectively showcases the enhancement in performance achieved by employing IED. The utility of range detection utilizing IED is discussed in [5]. [6]

¹Faculty of Technology, D. D. University, Gujarat 387001, INDIA. Email: nvc.ec@ddu.ac.in

²Faculty of Computer Science and Application, Charotar University, Changa, Gujarat, INDIA.

³Faculty of Technology, D. D. University, Gujarat 387001, INDIA.

proposes a solution for selecting the optimal power value, denoted as "p," in order to achieve the minimum overall error rate. Additionally, [6] investigates the performance of multi-antenna-based IED in cooperative SS, whereas the aforementioned studies mainly focus on static cognitive users. Furthermore, [7] assesses the performance of fading over IED in a cooperative network considering the static distance of users. [8] Evaluates the efficiency of ED in the presence of uncorrelated fading, accounting for imperfect CSI. However, in practical scenarios, the placement of antennas may be constrained due to space limitations, which can potentially impact the quality of the wireless link. To estimate the compatibility of multipath components at the receiver, common models such as uniform, random, and correlated fading are employed [9]. Reference [10] explores the performance of ED in the presence of randomly correlated Nakagami-m fading channels. The authors validate the detection performance of ED with ideal channel state information (CSI) by considering various user distances within a metropolitan network model. However, in practical scenarios, ideal CSI is typically not available, thus necessitating the evaluation of detection performance under imperfect CSI conditions [11–14]. Several studies in the literature have focused on modified threshold techniques within scenarios involving uncorrelated and limited users [15–19]. These studies aim to address the challenges posed by imperfect CSI and propose techniques to optimize the detection performance of ED in such scenarios. Applying a power-based operation using a value of p can be a valuable approach to enhance the performance of ED. Prior studies have established performance bounds for Uniform and

exponentially correlated fading, taking into account limitations imposed by imperfect CSI. In practical scenarios, the impact of inadequate CSI on the performance of IED at fixed distances can be significant. Combining the Static Threshold (ST) and Modified Threshold (MT) techniques can further enhance the effectiveness of ED. Furthermore, possessing statistical knowledge of the received signal-to-noise ratio (SNR) proves advantageous in mitigating the effects of antenna correlation and the static distance of secondary users [20–24]. Notably, as of now there is no any previous research which has proposed or investigated the impact of faulty CSI on Uniformly and Exponentially correlated MIMO over Nakagami-m fading employing MRC to evaluate the detection performance of IED. In this article, we contribute in the following ways:

1. We derive closed-form expressions for the probability of missed detection to assess the effectiveness of IED in a cognitive radio environment. To account for practical scenarios, we consider incomplete channel

state information. These derived expressions can also be applied for independent and identically distributed branches.

2. We evaluate the overall error rate of the same. Additionally, we investigate the impact of inter-branch correlation on the overall error rate.

The forthcoming version of the paper will exhibit:

- Section II: System Model, which provides a detailed description of the system model employed in our analysis.
- Section III: Performance of IED, where we demonstrate and discuss the performance characteristics of IED based on the derived expressions.
- Section IV: Simulation Results, where we present the numerical results obtained through simulations.
- Section V: Conclusion, which summarizes the main findings and concludes the paper.

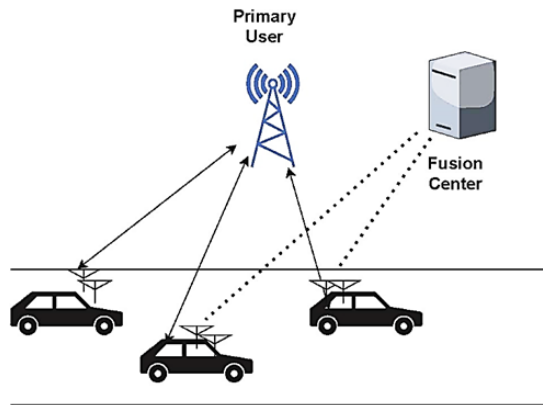


Fig 1. Network Model

Figure 1 depicts the model of a cognitive radio (CR) network in dense traffic scenarios, as considered in our study. The model consists of N unlicensed users, a licensed user located at 2-dimensional plane $p(x, y)$, and a Fusion Centre. Our assumption is that both the licensed user and Fusion Centre are equipped with an individual antenna respectively, while the unlicensed user possess “L” antennas. For signal combining, we employ Maximum Ratio Combining (MRC), which is a simpler technique compared to hybrid channel selection. By utilizing MRC, we can derive statistical information about the receiver signal-to-noise ratio (SNR) even in the presence of noisy CSI.

A. Static Distance Model:

The static distance of the secondary user (SU) introduces a time-selective fading characteristic. We adopt an autoregressive process to define the effect of the SU's static distance, as described in [7]. The coefficient of fading channel, denoted as “ h_j ”, for the two signalling instances can be numerically equated as:

$$h_j(\tau_1) = \rho_j h_j(\tau_2) + \sqrt{1 - \rho_j^2} e_j(\tau_1) \quad (1)$$

Where, $\rho_j = \mathcal{J}_0\left(\frac{2\pi f_c v_j}{R_s c}\right)$ is the correlation parameter that represents the gain of correlated time adjacent channel, and the remaining notation of the equation is referred from [7].

B. Channel Model:

To evaluate the yield of the cognitive radio, we consider the “Nakagami-m” channel and employ Maximum Ratio Combining (MRC) with Uniformly and Exponentially correlated antennas. Specifically, we examine the case of arbitrarily correlated “Nakagami-m fading” over MRC, as described in [25]:

$$p_{\gamma_{MRC}}(\gamma) = \frac{(1 - \rho)^m}{\Gamma(m)} \sum_{k=0}^{\infty} \frac{B\left(2(k+m), \frac{1}{2}\right) c^{2(k+m)} \rho^k}{k! \Gamma(k+m) 2^{2(k+m-1)}} \times \gamma^{2(k+m)-1} e^{-2c\gamma} {}_1F_1\left(2(k+m); 2(L+k+m) + \frac{1}{2}; c\gamma\right), \quad \gamma \geq 0$$

(2)

Here, $c = m/(\bar{\gamma}(1-\rho))$, $B(\alpha, \beta)$ denotes the beta function, m is the Nakagami- m parameter, and γ represents the instantaneous SNR. $1F1$ refers to the ‘‘Gaussian hypergeometric function’’, and L represents total antenna branches.

For the ‘‘Nakagami- m ’’ branches with exponentially correlated over MRC, the expression is given by [25] and references therein:

$$f(r_1, r_2, \dots, r_L) = \frac{r_1^{m-1} r_L^m}{2^{m-1} \Gamma(m) (1-\rho_1^2)^{m(L-1)}} e^{-\frac{r_1^2 + r_L^2}{2(1-\rho_1^2)}} g_1$$

(3)

where $g_1 = \begin{cases} 0, & \text{for } L = 2 \\ \frac{\rho^2 + 1}{2(1-\rho^2)} \sum_{k=2}^{L-1} r_k^2, & \text{for } L > 2 \end{cases}$, ρ_1 is correlation parameter for exponential.

C. Faulty CSI:

Considering the presence of fading links based on time selective. between the primary user and the secondary user, the signal received, denoted as ‘‘ sth ,’’ expressed as follows [7]:

$$y_j(s) = \underbrace{\rho_j^{s-1} h_j(1)x(s)}_{\text{desired signal}} + \underbrace{x(s) \phi_j(s)}_{\text{noise of node static distance}} + \underbrace{n_j(s)}_{\text{noise}}$$

(4)

To derive the received signal $y_j(s)$ as described in section 3, we rewrite the expression of h_j for the sth position of signaling as follows:

$$h_j(s) = \rho_j^{s-1} h_j(1) + \underbrace{\sqrt{1 - \rho_j^2} \sum_{l=1}^{s-1} \rho_j^{s-l-1} e_j(l)}_{\triangleq \phi_j(s)} \quad (5)$$

The cumulative noise power for the received signal, as described in [7], is defined by the following expression:

$$\sigma_{eff_j}^2 = (1 - \rho_j^{2(s-1)}) \sigma^2 E_s + \rho_j^{2(s-1)} \sigma_{\epsilon_j}^2 E_s + \sigma_{n_j}^2 \quad (6)$$

Here, $\sigma_{\epsilon_j}^2$ represents the variability of imperfect channel estimation, ranging from 0 to 1. The symbol energy is denoted as E_s .

D. Signal Model:

The binary hypothesis regarding the signal received at the j th secondary user (SU) can be expressed as Follows:

$$\begin{aligned} H_0: y_j(s) &= n_j(s) \\ H_1: y_j(s) &= \rho_j^{s-1} h_j(1)x(s) + x(s)\phi_j(s) + n_j(s) \end{aligned} \quad (7)$$

In this context, H_0 represents the absence of the primary user (PU) signal, while H_1 signifies the presence of the PU signal. The decision statistics for the j th SU using the Improved Energy Detector (IED) at the sth instant are provided in [7].

$$W_j \triangleq \frac{2}{N_0} \int_0^T |y_j(s)|^p dt, p > 0 \quad (8)$$

In the above equation, p represents the arbitrary power parameter for the IED, and W_j refers to the decision statistic for the observation at the sth instant at the j th SU. It is important to note that if we substitute p with the squaring operation, W_j will reduce to the level associated with ED.

2. Performance of IED Over Correlated Nakagami-M Fading Under Threshold Verification

We calculate missed detection probability by deriving the Probability Density Function under the H_0 and H_1 hypotheses. PDF under H_0 and H_1 hypothesis.

The PDF of the Signal-to-Noise Ratio (SNR) under the H_0 hypothesis, considering additive white Gaussian noise, is expressed as:

$$f_{W_j|H_0}(y_j) = \frac{1}{p\Gamma(u)2^{u-1}} y_j^{\frac{2u}{p}-1} \exp\left(-\frac{y_j^{\frac{2}{p}}}{2}\right)$$

(9)

To calculate the missed detection probability over MRC, we obtain the PDF under the H_1 hypothesis as follows [8, Eq. 20]:

$$f_{W_y | H_1}(z) = \frac{4z^{\frac{2-p}{p}} \exp\left(-\frac{z^{\frac{2}{p}}}{p^{2(k-1)}}\right) + \sigma_{eff}^2}{p(p^{2(k-1)} + \sigma_{eff}^2)} \times \left(1 - \exp\left(-\frac{z^{\frac{2}{p}}}{p^{2(k-1)} + \sigma_{eff}^2}\right)\right)$$

(10)

A. Pm with Modified Threshold:

The probability of missed detection with Modified Threshold is expressed as follows:

$$P_m = \int_{-\infty}^{\lambda} f_{W_j|H_1}(z) f_z(z) dz$$

(11)

By substituting equation (2) into equation (11), the integral term for the missed detection probability over a uniformly distributed Nakagami- m channel can be expressed as:

$$P_m = \int_{-\infty}^1 \frac{4z^{\frac{2-p}{p}} \exp\left(-\frac{z^{\frac{2}{p}}}{\rho^{2(k-1)}}\right) + \sigma_{eff}^2}{p(\rho^{2(k-1)} + \sigma_{eff}^2)} \times \left(1 - \exp\frac{\frac{z^2}{p}}{\rho^{2(k-1)} + \sigma_{eff}^2}\right) \times z^{2(m+k)-1} e^{-2cz} {}_1F_1\left(2(m+k); 2(m+k) + \frac{1}{2}; cz\right) \times \frac{(1-\rho)^m}{\Gamma(m)} \sum_{k=0}^{\infty} \frac{B\left(2(m+k), \frac{1}{2}\right) c^{2(m+k)} \rho^k}{k! \Gamma(m+k) 2^{2(m+k-1)}} dz$$

To further analyze the aforementioned integral, let us consider:

$$t = \left(1 - \exp\frac{-z^{2/p}}{\rho^{2(k-1)} + \sigma_{eff}^2}\right)$$

so that,

$$dt = \frac{2z^{(2-p)/p} \exp\left(-z^{2/p}/(\rho^{2(k-1)} + \sigma_{eff}^2)\right)}{p(\rho^{2(k-1)} + \sigma_{eff}^2)} dz$$

For P_m , it is suggested to use equation (15) by adjusting the bounds and solving the integral using software such as Mathematica. Special integral rules described in [27] can be applied, and constants within the integral can be removed or simplified. The Lauricella hypergeometric function can be denoted by the symbol F_1 .

Similarly, in the case of Exponential correlation, the likelihood of missing a detection can be expressed as follows:

$$P_{m1} = \int_{-\infty}^{\lambda} \frac{4z^{(2-p)/p} \exp\left(-z^{2/p}/\rho^{2(k-1)}\right) + \sigma_{eff}^2}{p(\rho^{2(k-1)} + \sigma_{eff}^2)} \times \left(1 - \exp\frac{z^2/p}{\rho^{2(k-1)} + \sigma_{eff}^2}\right) \times \frac{z^{m-1} z^m}{2^{m-1} \Gamma(m) (1-\rho_1^2)^{m(n-1)}} e^{-\frac{z^2+z^2}{2(1-\rho_1^2)} g_1} dz$$

(12)

The missed detection probability can be calculated using equation (18), where l_1 , l_2 , and l_3 are defined as ρ_1^{2L-1} , mg , and λk , respectively. The term Ku represents Kummer's solution, as described in [27], with z_1 , z_2 , and z_3 denoting $\Gamma(2L-1)$, λ , and γ , respectively.

Refer Appendix ■

B. Total Error Rate Analysis Under MT:

FC calculates the overall error rate of CR Network. Binary decision broadcasted by each SU, indicating the presence

or absence of the PU which is based on the decision rule outlined in [7]. These individual decisions from N SUs are then transmitted to the FC, but the reporting channel may introduce errors. Consequently, N binary decisions are obtained. The total error rate Q , taking into account the imperfections in the reporting channel, can be computed as described as:

$$Q \triangleq \beta E_f + (1 - \beta) E_m$$

(13)

The equation represents the required error rate, Q , which gets influenced by both the likelihood of false alarm, E_f , and the probability of missed detection, E_m , at the FC. The probabilities of the prior information for hypotheses H_0 and H_1 are denoted as β and $(1 - \beta)$ respectively, as indicated in equation (13). In the context of the investigated dense traffic CR Network model, an equiprobable hypothesis is considered, with $\beta = 0.5$, to reflect the overall error rate.

$$E_f = 1 - [(1 - P_f)(1 - \epsilon) + \epsilon P_f]^N$$

$$E_m = [P_m(1 - \epsilon) + \epsilon(1 - P_m)]^N$$

(14)

To calculate the overall error rate, we consider $N = 2$. The values for the probability of missed detection, E_m , and the probability of false alarm, E_f , are obtained from equations (16) and (17) respectively. The error probability is defined as ϵ .

3. Pm Analysis for Uniform Dand Exponential With Mimo System

In this section, we focus on deriving the missed detection probability for the Uniform and Exponential correlated MIMO configurations. These derived expressions are valuable in assessing the significance of the MT. Through an analytical approach, we obtain closed-form expressions for the missed detection probability in the Uniform and Exponential correlated MIMO configurations using traditional methods. Equations 19 to 28 present the specific expressions for the missed detection probability.

$$P_m = \frac{1}{2(1 - \exp(M))^2} \times k_{\mu}(z_1, z_2, z_3)$$

(15)

$$E_m = 0.5(1 - \exp(M))^2 \times (1 - \epsilon) + \epsilon - 0.5(1 - \exp(M))^2$$

(16)

Where,

$$M = \frac{\lambda^{\frac{2}{p}}}{1 + \lambda p_j^{(2(k-1))} + F_1(p^{2k-1}, m, k) + p^{(2(k-1))\sigma^2_{eff}}} \sigma^2 n$$

$$E_f = 1 - \left(\frac{1}{2} - \frac{1}{2} \left(1 - \exp \frac{-\lambda^{\frac{2}{p}}}{\sigma_n^2} \right)^2 \times (1 - \epsilon) \right) - \left(\frac{1}{2} - \frac{1}{2} \left(1 - \exp \frac{-\lambda^{2/p}}{\sigma_n^2} \right)^2 \times (1 - \epsilon) \right)$$

(17)

$$P_{m1} = \left(1 - \exp \left(\frac{1}{1 + \lambda \rho_j^{(2(k-1))} + \rho_1^{(2(k-1))} \sigma_{eff}^2} \sigma_n^2 \right) \right)^2 \times F_1(l_1, l_2, l_3)$$

(18)

$$W = \int_0^\infty \int_{-\infty}^{yz} \frac{d}{4ab} \left(\pi + 2 \arcsin \left(\frac{2(y^2 - (d'')^2)}{y^2} \right) \right)$$

(19)

$$X = \frac{2^{4m-4-i_1-i_2} \Gamma \left(\frac{1}{2(4m+2k_1+i_2-2k_2-2-i_1)} \right)}{\Gamma(4(m-1))} \times \frac{\Gamma(1/2(i_1-2k_1+2k_2+4m))}{\Gamma(1/2(2m-i_1-i_2))} dx dy$$

(20)

$$P_m(MIMO) = W \times X$$

(21)

$$Y = k B_k \sum_{n=1}^{T_k} \lambda_k^n m z^m \frac{e^{h_p \eta / ab} (1/ab)}{d^2}$$

(22)

$$Z = \frac{2^{4m-4-i_1-i_2} \Gamma \left(\frac{1}{2(4m+2k_1+i_2-2k_2-2-i_1)} \right)}{\Gamma(4(m-1))} \times \frac{\Gamma(1/2(i_1-2k_1+2k_2+4m))}{\Gamma(1/2(2m-i_1-i_2))}$$

(23)

$$P_m(MRC) = Y + Z$$

(24)

$$Q_1 = \frac{2^{4m-4-i_1-i_2} \Gamma \left(\frac{1}{2(4m+2k_1+i_2-2k_2-2-i_1)} \right)}{\Gamma(4(m-1))} \times \frac{\Gamma(1/2(i_1-2k_1+2k_2+4m))}{\Gamma(1/2(2m-i_1-i_2))}$$

(25)

$$P_m(U_{ni}) = \sum_{i_1=0}^{m-1} \sum_{k_1=1}^{i_1} \sum_{i_2=0}^{m-1} \sum_{k_2=0}^{i_2} \binom{m-1}{i_1} \binom{i_1}{k_1} \binom{m-1}{i_2} \binom{i_2}{k_2} \times A_k \times B_k \sum_{n=1}^{T_k} d_k^n m z^m \frac{e^{\frac{h_p n}{ab}} \left(\frac{1}{ab} \right)}{d^2}$$

(26)

Q_2

$$= \frac{K_{22} 8 \pi^{\frac{5}{2}} 2^{4m-4-i_1-i_2} \Gamma \left(\frac{1}{2(4m+2k_1+i_2-2k_2-2-i_1)} \right)}{2^{2m-1} \Gamma(4(m-1))} \times \frac{\Gamma(1/2(i_1-2k_1+2k_2+4m))}{\Gamma(1/2(2m-i_1-i_2))}$$

(27)

$P_m(Exp)$

$$L r^{\pi \frac{\mu_x + \mu_y}{2}} \sum_{k=0}^{\infty} \frac{k! m_k L_k^{\frac{\mu_x + \mu_y}{2}} \left(\left(\frac{2}{\mu_x + \mu_y} + 1 \right) 2 r^\alpha \right)}{\left(\frac{\mu_x + \mu_y}{2} + 1 \right)_k} = \frac{2^{\frac{\mu_x + \mu_y}{2} + 1} \Gamma \left(\frac{\mu_x + \mu_y}{2} + 1 \right) \exp \left(\frac{r \pi}{2} \right)}{\times Q_2}$$

(28)

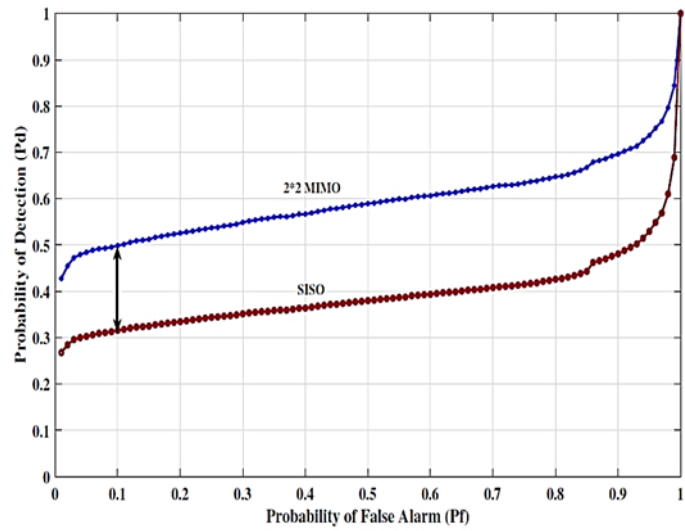


Fig 2. Pd against Pf between SISO and MIMO

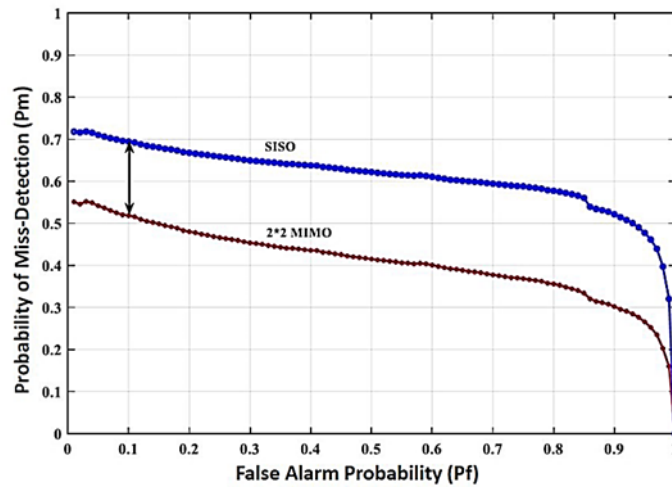


Fig 3. Pm against Pf between SISO and MIMO

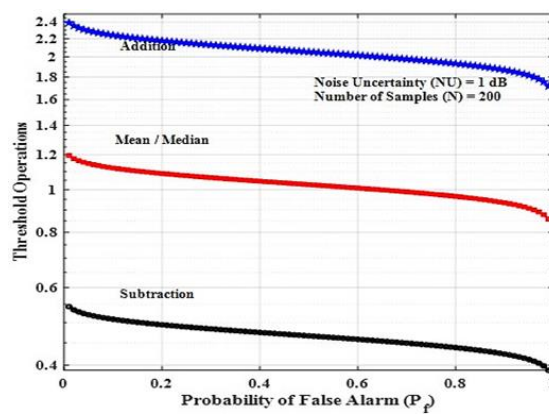


Fig 4. Threshold Operation against Pf

4. Numerical Results

The detailed analysis of these results can be found in our pre-print papers [28] and [29]. However, in this section, we validate our analysis by conducting Monte Carlo simulations. These simulations provide valuable insights into the design and implementation of CR systems with threshold operations. We performed the simulations using MATLAB, with a total of 10^8 simulation runs. Various first-order performance metrics, such as the probability of false alarm and detection probability, were identified and evaluated. Specifically, we focused on assessing the performance of the Uncorrelated, Uniform correlation, Exponential correlation, MRC with

Exponential correlation, and MIMO systems using the MT.

Figure 4 illustrates the relationship between threshold operations and false alarms. The results show that as the false alarm rate increases, the magnitude of the threshold decreases. The mean, addition, and subtraction operations are compared in this analysis. Interestingly, it is observed that these operations provide equal margin gains for certain false alarm values. This suggests that, for 5G and beyond systems, selecting the lowest and optimal false alarm value becomes crucial in determining the most suitable threshold operation to perform.

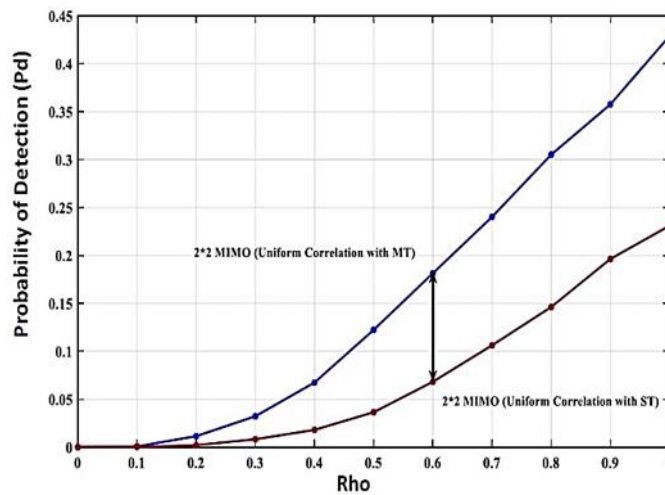


Fig 5. Pd against Correlation Coefficient (Rho) with ST and MT

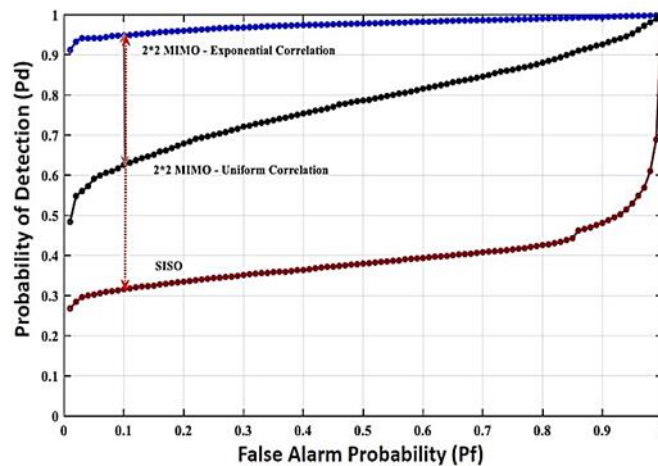


Fig 6. Pd against Pf with MT for SISO and Correlated MIMO

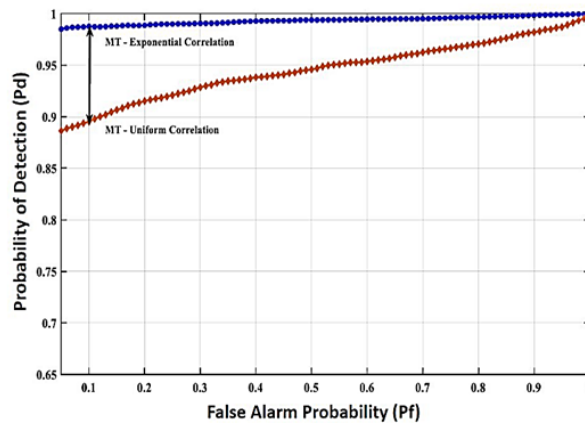


Fig 7. Pd against Pf with MT for Correlated MIMO over MRC

Figure 9 presents the detection probability as a function of the signal-to-noise ratio (SNR) for both single-input single-output (SISO) and multiple-input multiple-output (MIMO) systems. The results clearly demonstrate that the utilization of the MT significantly enhances the detection probability. Specifically, at low SNR values, such as -20dB, the MT plays a crucial

role in correctly identifying the samples of the detected signal. This underscores the importance of the threshold operations and their impact on the overall detection performance. This highlights the superior performance of the modified threshold in detecting signals under challenging conditions.

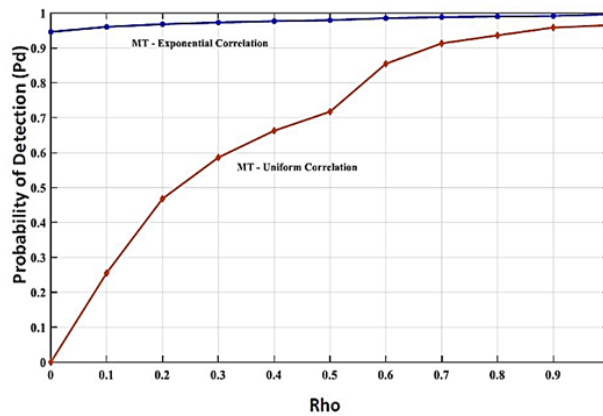


Fig 8. Pd against Rho with MT for Correlated MIMO over MRC

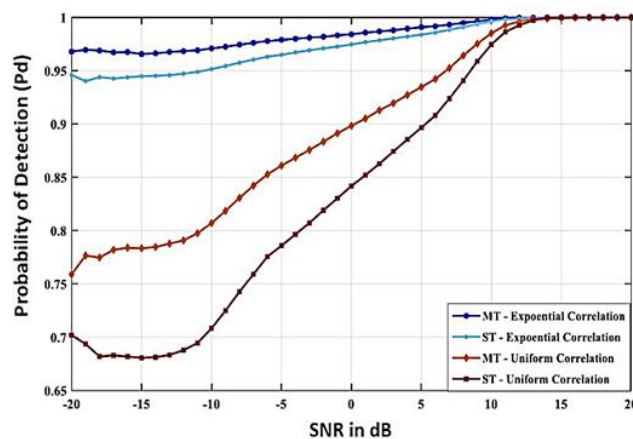


Fig 9. Pd against SNR with MT for Correlated MIMO over MRC

Furthermore, Figure 6 emphasizes the significance of the MT in MIMO systems. In contrast to SISO systems, the MT often improves the performance of MIMO systems with dual antennas, particularly in the low SNR regime. This suggests that the utilization of multiple

antennas can effectively mitigate the adverse effects of deep fading, leading to a more reliable detection of the signal.

Figure 2 illustrates a comparison between SISO and MIMO configurations using the MT in terms of false

alarm rates. The plot represents the detection probability as a function of the false alarm rate. The results clearly demonstrate the importance of the MT in both SISO and MIMO configurations. It is observed that as the false alarm rate approaches unity (i.e., a high probability of

false alarm), the detection probability also tends towards unity. This validates the expected behavior of false alarm rates and their impact on the overall detection performance in both SISO and MIMO systems.

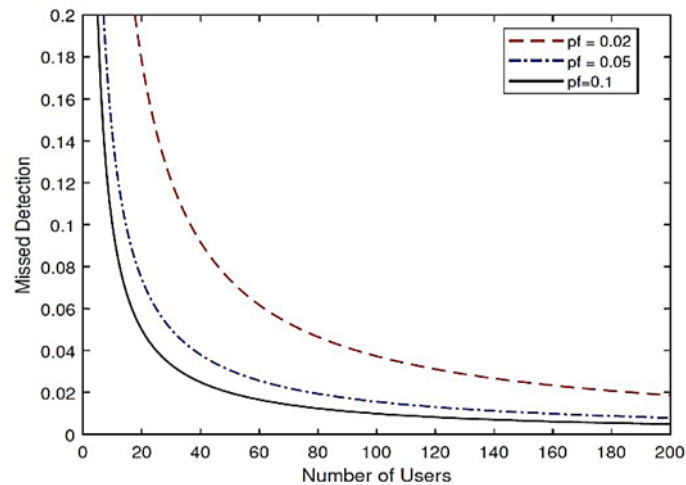


Fig 10. Pm against Users

Figure 3 presents a comparison between SISO and MIMO configurations using the MT. The plot shows the missed detection probability as a function of the false alarm rate. The results clearly indicate the significance of the modified threshold in both configurations. It also demonstrates the consistent improvement achieved through the threshold operations. Considering that wireless communication channels are subject to continuous broadcasting, employing MIMO design with the modified threshold can be an effective solution for detecting the PU and mitigating deep fades. The study further confirms the behavior of false alarm rates, showing that as they approach unity, the missed detection probability approaches zero.

Figure 7 to Figure 9 provide insights into the significance of the MT for MIMO systems and correlated systems. These figures demonstrate the improvements in detection probability achieved by applying robust numerical methods to the threshold operation. It is worth noting that the numerical methods employed do not compromise the performance of the IED by introducing analytical loops. This implies that the performance of the IED relies on factors such as the non-linearity parameter of the fading channel and the spacing between antennas.

Figure 10 focuses on missed detection probability in relation to the number of users, aiming to enhance the usage of an effective SS technique. The plot reveals that as the number of users increases, the detection performance for SS in CR networks improves. This highlights the importance of considering multiple users

in the detection process and the potential benefits of leveraging advanced SS techniques.

5. Conclusion

We assess the performance of an ED in a vehicular network using dual antennas at the SU. Specifically, we evaluate the ED's performance over both evenly and exponentially correlated Nakagami-m fading channels, considering the MT approach. We calculate the likelihood of missed detection using MRC diversity scheme.

Our analysis takes into account various factors that can impact the ED performance in vehicular networks, including the static distance between SUs, imperfect CSI, and antenna correlation. We find that faulty CSI can lead to a reduction in detection performance, particularly at the same relative distance. Furthermore, the overall error rate is influenced by both antenna correlation and the static distance of the SUs. Interestingly, we observe that exponential correlation yields superior performance compared to linear correlation. This suggests that incorporating exponential correlation can enhance the ED's ability to detect primary users. Importantly, we note that the use of the MT approach does not negatively affect the natural behavior of the system, demonstrating its compatibility and effectiveness.

VI .APPENDIX - ANALYSIS OF MISSED DETECTION PROBABILITY

In this section, we focus on calculating the missed detection probability for the ED over a Uniformly correlated Nakagami-m fading channel. To do this, we

evaluate the internal terms of the integral involved in the calculation. By removing the constants from the integral and performing specific mathematical manipulations, we can represent the integral terms using a specific integral rule provided in [27].

$$P_m = \int_{-\infty}^{\lambda} \frac{4z^{(p-2)/p} \exp(-z^{2/p}/\rho^{(2k-1)}) + \sigma_{eff}^2}{p(\rho^{2(k-1)} + \sigma_{eff}^2)} dz$$

(29)

We keep the constant outside and further solving:

$$P_m = \left\{ \frac{1}{2} i^{(3-p)p} p \left(\Gamma\left(-\frac{1}{2}(p-3)p\right) - \Gamma\left(-\frac{1}{2}(p-3)p, -10000^{1/p}\right) \right), 0 < \Re(p) < 3 \right.$$

(30)

Equation (15) is derived by simplifying Equation (30) using the identity given in [26, Section 8]. By substituting Equation (3) into Equation (11) for an exponentially correlated Nakagami-m fading, we obtain the expression for the missed detection probability, which is given by Equation (15).

References

[1] M. Vegni and D. P. Agrawal, *Cognitive Vehicular Networks*. CRC Press, 2016.

[2] H. Urkowitz, "Energy detection of unknown deterministic signals," *Proc. IEEE*, vol. 55, no. 4, pp. 523–531, 1967.

[3] T. Yucek and H. Arslan, "A survey of spectrum sensing algorithms for cognitive radio applications," *IEEE Commun. Surveys & Tuts.*, vol. 11, no. 1, pp. 116–130, 2009.

[4] Y. Chen, "Improved energy detector for random signals in Gaussian noise," *IEEE Trans. Wireless Commun.*, vol. 9, no. 2, pp. 558–563, 2010.

[5] A. Singh, M. R. Bhatnagar, and R. K. Mallik, "Cooperative spectrum sensing with an improved energy detector in cognitive radio network," in *Proc. of IEEE NCC*, 2011, pp. 1–5.

[6] A. Singh, M. R. Bhatnagar, and R. K. Mallik, "Cooperative spectrum sensing in multiple antennas based cognitive radio network using an improved energy detector," *IEEE Commun. Lett.*, vol. 16, no. 1, pp. 64–67, January 2012.

[8] L. Gahane, P. K. Sharma, N. Varshney, T. A.

Tsiftsis, and

[9] P. Kumar, "An improved energy detector for mobile cognitive users over generalized fading channels," *IEEE Trans. Commun.*, vol. 66, no. 2, pp. 534–545, 2017.

[10] L. Gahane and P. K. Sharma, "Performance of improved energy detector with cognitive radio mobility and imperfect channel state information," *IET Commun.*, vol. 11, no. 12, pp. 1857–1863, 2017.

[11] V. A. Aalo, "Performance of maximal-ratio diversity systems in a correlated Nakagami-fading environment," *IEEE Trans. Commun.*, vol. 43, no. 8, pp. 2360–2369, 1995.

[14] S. Kavaiya, D. K. Patel, Y. L. Guan, S. Sun, Y. C. Chang,

[15] and J. M. Lim, "On the energy detection performance of arbitrarily correlated dual antenna receiver for vehicular communication," *IEEE Commun. Lett.*, vol. 23, no. 7, pp. 1186–1189, July 2019.

[16] H. S. Abed and H. N. Abdullah, "Improvement of spectrum sensing performance in cognitive radio using modified hybrid sensing method," *Acta Polytechnica*, vol. 62, no. 2, pp. 228–237, 2022.

[18] S. S. Chopade and S. S. Dalu, "Improving security with optimized qos in cognitive radio networks using ai backed blockchains," in *ICCCE 2021*. Springer, 2022, pp. 629–638.

[20] P. Skokowski, K. Malon, and J. Łopatka, "Building the electromagnetic situation awareness in manet cognitive radio networks for urban areas," *Sensors*, vol. 22, no. 3, p. 716, 2022.

[22] N. Chaudhary and R. Mahajan, "Comprehensive review on spectrum sensing techniques in cognitive radio," *Engineering Review: 42(1)*, 88–102, <http://doi.org/10.30765/er.1677>, vol. 42, no. 1, pp. 0–0, 2022.

[25] S. Madbushi and M. Rukmini, "Mitigation of primary user emulation attack using a new energy detection method in cognitive radio networks," *Journal of Central South University*,

vol. 29, no. 5, pp. 1510–1520, 2022.

- [26] H. S. Abed and H. N. Abdullah, “Improvement of spectrum
- [27] sensing performance in cognitive radio using modified hybrid sensing method,” *Acta Polytechnica*, vol. 62, no. 2, pp. 228–237, 2022.
- [28] S. Murugan Suganthi and G. Ramaswamy Shunmugavel, “Improved hard fusion methods for enhancing detection and energy efficiency in cognitive radio networks,” *Concurrency and Computation: Practice and Experience*, vol. 34, no. 5, p. e6686, 2022.
- [29] X. Zhang, N. Chen, N. Zhao, Y. Luo, W. Kan, and S. Yang,
- [30] “Spectrum allocation and power control in OFDM systems for cognitive radio networks,” in *2022 9th international Conference on Wireless Communication and Sensor Networks (ICWCSN)*, 2022, pp. 57–64.
- [31] M. Shili, M. Hajjaj, and M. L. Ammari, “User clustering and power allocation for massive mimo with noma-inspired cognitive radio,” *IEEE Transactions on Vehicular Technology*, 2022.
- [32] A. Kumar, P. Thakur, S. Pandit, and G. Singh, “Analysis of optimal threshold selection for spectrum sensing in a cognitive radio network: an energy detection approach,” *Wireless Networks*, vol. 25, no. 7, pp. 3917–3931, 2019.
- [33] B. Sarala, S. R. Devi, and J. J. J. Sheela, “Spectrum energy detection in cognitive radio networks based on a novel adaptive threshold energy detection method,” *Computer Communications*, vol. 152, pp. 1–7, 2020.
- [34] W. Wu, Z. Wang, L. Yuan, F. Zhou, F. Lang, B. Wang, and
- [35] Q. Wu, “Irs-enhanced energy detection for spectrum sensing in cognitive radio networks,” *IEEE Wireless Communications Letters*, vol. 10, no. 10, pp. 2254–2258, 2021.
- [36] S. Yu, J. Liu, J. Wang, and I. Ullah, “Adaptive double-threshold cooperative spectrum sensing algorithm based on history energy detection,” *Wireless Communications and Mobile Computing*, vol. 2020, pp. 1–12, 2020.
- [37] Li, Xingwang, Yu, Shanshan, Wang, Jing, and Ullah, Inam “Adaptive double-threshold cooperative spectrum sensing algorithm based on history energy detection,” *Wireless Communications and Mobile Computing*, vol. 2020, pp. 1–12, 2020.
- [38] S. Al-Juboori and X. N. Fernando, “Multiantenna spectrum sensing over correlated Nakagami- m channels with MRC and EGC diversity receptions,” *IEEE Trans. Veh. Technol.*, vol. 67, no. 3, pp. 2155–2164, 2018.
- [39] I. S. Gradshteyn and I. M. Ryzhik, *Table of integrals, series, and products*. Academic press, 2014.
- [40] A. D. Rich and D. J. Jeffrey, “A knowledge repository for indefinite integration based on transformation rules,” in *Proc. ICICM*. Springer, 2009, pp. 480–485.
- [41] N. Chauhan, “Performance Enhancement of Multi-antenna Correlated Receiver for Vehicular Communication using Modified Threshold Approach”. TechRxiv, 07-Apr-2023.
- [42] Chauhan, Narendrakumar (2023). Performance Enhancement of Multi-antenna Correlated Receiver for Vehicular Communication using Modified Threshold Approach. TechRxiv.preprint. <https://doi.org/10.36227/techrxiv.22559176.v1>